Benefits analysis of Soft Open Points for electrical distribution network operation

Wanyu Cao [a], Jianzhong Wu [a,*], Nick Jenkins [a], Chengshan Wang [b], Timothy Green [c]

[a] Institute of Energy, School of Engineering, Cardiff University, Cardiff CF24 3AA, UK
[b] Key Laboratory of Smart Grid of Ministry of Education, Tianjin University, Tianjin 300072, China
[c] School of Engineering, Imperial College London, London, UK

HIGHLIGHTS

- An analysis framework was developed to quantify the operational benefits.
- The framework considers both network reconfiguration and SOP control.
- Benefits were analyzed through both quantitative and sensitivity analysis.

ARTICLE INFO

ABSTRACT

Soft Open Points (SOPs) are power electronic devices installed in place of normally-open points in electrical power distribution networks. They are able to provide active power flow control, reactive power compensation and voltage regulation under normal network operating conditions, as well as fast fault isolation and supply restoration under abnormal conditions. A steady state analysis framework was developed to quantify the operational benefits of a distribution network with SOPs under normal network operating conditions. A generic power injection model was developed and used to determine the optimal SOP operation using an improved Powell's Direct Set method. Physical limits and power losses of the SOP device (based on back to back voltage-source converters) were considered in the model. Distribution network reconfiguration algorithms, with and without SOPs, were developed and used to identify the benefits of using SOPs. Test results on a 33-bus distribution network compared the benefits of using SOPs, traditional network reconfiguration and the combination of both. The results showed that using only one SOP achieved a similar improvement in network operation compared to the case of using network reconfiguration with all branches equipped with remotely controlled switches. A combination of SOP control and network reconfiguration provided the optimal network operation.

© 2016 The Authors. Published by Elsevier Ltd. This is an open access article under the CC BY license (http://creativecommons.org/licenses/by/4.0/).

1. Introduction

The widespread use of distributed energy resources, e.g., distributed generators (DG), energy storage and controllable loads, is being promoted by many countries. This can lead to operation problems including excessive fault level as well as violations of thermal and voltage limits [1,2]. Power utilities have conventionally used expensive and time consuming approaches such as building new circuits to maintain the quality of power supply. However, there are also alternative operational measures being investigated, aiming at reliable and cost-efficient operation of distribution networks [3], e.g., network reconfiguration and increasing use of power electronic devices.

In a distribution network, there are usually a number of normally-open points connecting adjacent feeders. These normally-open points (switches) are able to be closed (while opening other switches) to reconfigure the network and achieve load transfer between feeders. Under normal operating conditions, extensive research has been conducted into network reconfiguration for optimal network operation (e.g., load balancing, loss minimization and improved voltage profiles) [4,5]. However, practical applications of automatic network reconfiguration are presently very limited due to the high cost of remotely-controlled switches, the associated ICT (information and communication technologies) infrastructure, and maintenance of hardware/software.

* Corresponding author.
E-mail addresses: CaoW5@Cardiff.ac.uk (W. Cao), WuJ5@cardiff.ac.uk (J. Wu), JenkinsN6@cardiff.ac.uk (N. Jenkins), cswang@tju.edu.cn (C. Wang), t.green@imperial.ac.uk (T. Green).

An alternative solution to improve distribution network operation, without requiring network topology changes, is the use of power electronic devices. Power electronic devices enable more efficient use of existing network capacity by controlling power flows in an accurate and flexible way [6]. A wealth of information exists on the use of these devices in the transmission network for bulk power transfer [7]. Recently, installing power electronic devices in place of normally-open points in a distribution network, namely 'Soft' Open Points (SOPs), has been investigated [8,9]. Instead of simply opening/closing normally-open points, these devices are able to control load transfer and optimize network voltage profile by providing fast, dynamic and continuous real/reactive power flow control between feeders [8].

Previous studies have investigated the use of power electronic devices at the normally-open points to facilitate distribution network operation [10,11]. In [10], a unified power flow controller was developed to regulate network voltage with minimum line losses in a simple loop network (with two feeders), and experimental results were presented to verify its effectiveness. Field tests of installing back-to-back converters between adjacent feeders were reported in [11]. Power flow was balanced which in turn led to reduced line losses and improved network voltages. Although the benefits of installing individual SOP for network operation have been investigated in a simple two-feeder network together with the controller design and simulation, methodologies for benefit quantification, i.e., steady state analysis of distribution networks with SOPs were not addressed and the advantages of the more widespread use of these devices in distribution networks have not been explored.

To fill this gap, a method to quantify the operational benefits of a distribution network with SOPs was developed, for power loss minimization, feeder load balancing and voltage profile improvement. A generic model of an SOP for steady state analysis was developed, which takes into account both physical limitations and internal power losses of the back-to-back voltage-source converters of a typical SOP device. Based on the SOP model, an improved Powell's Direct Set method was developed to obtain the optimal SOP operation. This method determines a good initial approximation of the SOP operation based on simplified power flow equations, which significantly reduces the computation burden. The performance of traditional network reconfiguration was compared to using SOPs. A method that combines SOP control and network reconfiguration was developed to identify the benefits. In addition, the benefits of using SOPs in distribution networks with DG connections were also investigated.

2. Steady state analysis of Soft Open Points

Fig. 1a shows a typical location of an SOP which allows the power electronic device to control active power flow between connected feeders and supply or absorb reactive power at its interface terminals under normal operation conditions.

2.1. Modeling of Soft Open Points

A generic power injection model of SOP was developed. This model considers SOP terminal power injections and hence enables straightforward incorporation of SOPs into existing power flow analysis algorithms without considering the detailed controller design.

Fig. 1b shows the representation of an SOP model with real and reactive power, injecting into feeders I and J through both terminals. Taking these power injections as decision variables, the power flow in feeder I is calculated by the following set of recursive equations [12]:

$$P_i = P_{i-1} - P_{Loss(i-1,i)} - P_{L,i} = P_{i-1} - \frac{r_{i-1}}{|V_{i-1}|^2} \cdot \left(P_{i-1}^2 + Q_{i-1}^2 \right) - P_{L,i}$$

(1.i)

$$Q_i = Q_{i-1} - Q_{Loss(i-1,i)} - Q_{L,i} = Q_{i-1} - \frac{x_{i-1}}{|V_{i-1}|^2} \cdot \left(P_{i-1}^2 + Q_{i-1}^2 \right) - Q_{L,i}$$

(1.ii)

$$|V_i|^2 = |V_{i-1}|^2 - 2 \cdot (r_{i-1}P_{i-1} + x_iQ_i) + \frac{(r_{i-1}^2 + x_{i-1}^2)}{|V_{i-1}|^2} \cdot \left(P_{i-1}^2 + Q_{i-1}^2 \right)$$

(1.iii)

with boundary conditions:

$$\left| P_n + P_{S\_inj}^I \right| = P_{Loss(n,sI)}$$

(2)

$$\left| Q_n + Q_{S\_inj}^I \right| = Q_{Loss(n,sI)}$$

(3)

where P represents active power, Q reactive power, V nodal voltage, r resistance and x reactance. Subscript $Loss$ denotes line losses, and L denotes load. The variables and parameters are shown in Fig. 1b. Similar recursive power flow equations with boundary conditions are applied to feeder J.

To consider the internal losses of the SOP equipment, the following equality constraint of power balance is used:

$$P_{S\_inj}^I + P_{S\_inj}^J + P_{SOP,Loss} = 0$$

(4)

where $P_{SOP,Loss}$ denotes the internal power losses of the whole SOP device.

Various types of power electronic devices can be implemented as an SOP, such as unified power-flow controllers, back to back and multi-terminal voltage-source converters [9]. In this paper, the back-to-back voltage-source converters (back-to-back) were
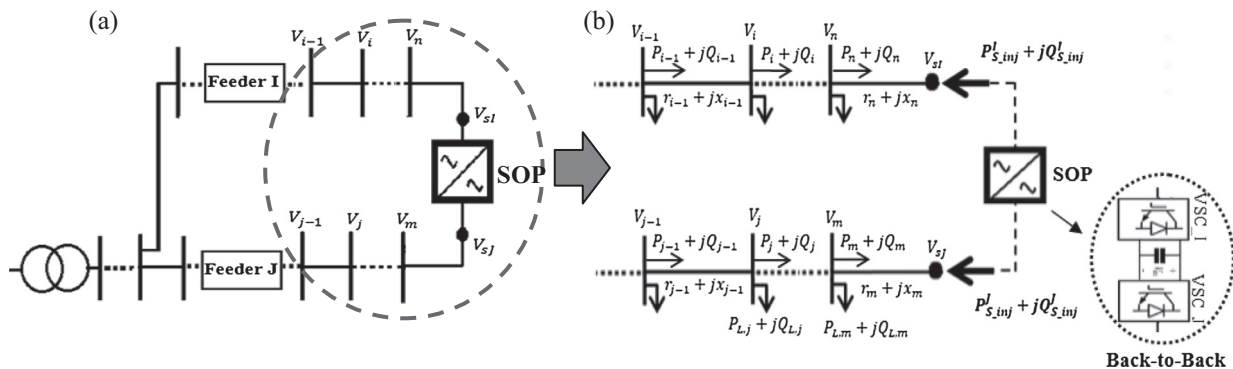

Fig. 1. (a) Simple distribution network with an SOP and (b) power injection model of SOP for distribution network power flow control.

used as an SOP. Constraints of such device due to the physical limitations and the internal power losses are formulated as follows.

2.1.1. Physical limitations of back-to-back converters

Back-to-back voltage-source converters consist of two insulated gate bipolar transistor (IGBT)-based voltage-source converters (VSCs). The two VSCs are series-connected on their DC sides, i.e., sharing a common capacitor, as shown in Fig. 1b. Both VSCs build their own voltage waveforms with desired amplitude and phase angle. This, in turn, gives a full (four-quadrant) control of the active power flowing through the dc link as well as independent reactive power supply or absorption at both interface terminals. A full description of the back-to-back converters properties can be found in [13].

The terminal power injections of back-to-back converters implemented as a SOP are controlled directly by each VSC, the operational limits of VSC capacity and terminal voltage are considered as:

$$\sqrt{P_{S\_inj}^{I}{}^{2} + Q_{S\_inj}^{I}{}^{2}} \leqslant S_{VSC,rate}^{I} \tag{5}$$

$$V_{sI} \leqslant V_{VSC,rate}^{I} \tag{6}$$

where $S_{VSC,rate}^{I}$ is the power rating of the VSC connected to feeder I; V_{sI} and $V_{VSC,rate}^{I}$ denote the actual and maximum ac terminal voltage. Similar capacity and terminal voltage constraints are applied to the other side VSC connected to feeder J.

2.1.2. Internal power losses of back-to-back converters

Internal power losses of the whole back-to-back device are made up of the losses of its individual components, including the semiconductors (conduction and switching losses), passive components (DC link capacitor, filter, AC line choke), transformers and the cooling system.

As suggested in [14], these losses can be categorized into three components: no load losses, linear and quadratic losses depending on the converter current, which is a function of the active and reactive power exchanged with the ac network:

$$P_{VSC,Loss}^{I} = a^{I} \cdot I_{VSC}^{I}{}^{2} + b^{I} \cdot I_{VSC}^{I} + c^{I} \tag{7}$$

$$I_{VSC}^{I} = \sqrt{P_{S\_inj}^{I}{}^{2} + Q_{S\_inj}^{I}{}^{2}} \Big/ |V_{sI}| \tag{8}$$

where $P_{VSC,Loss}^{I}$ and I_{VSC}^{I} represent the power losses and the ac current of the VSC connecting to feeder I. Similar equations are applied to the other side VSC. Thus all equations shown in the following section only illustrate the VSC connected to feeder I.

As shown in (7), the total losses are determined by the coefficients, a^{I}, b^{I} and c^{I}. These coefficients are difficult to obtain due to the limited information available from the open literature or manufacturers. Usually only the internal power losses (or efficiency) under nominal conditions and the no load loss, c^{I} are given. A linear function is used to approximate the quadratic one in (7):

$$P_{VSC,Loss}^{I} = k^{I} \cdot I_{VSC}^{I} + c^{I} \tag{9}$$

$$k^{I} = \left(P_{VSC,Loss,rate}^{I} - c^{I} \right) \Big/ I_{VSC,rate}^{I} \tag{10}$$

where $P_{VSC,Loss,rate}^{I}$ and $I_{VSC,rate}^{I}$ are power losses and ac current of the VSC connected to feeder I under nominal condition.
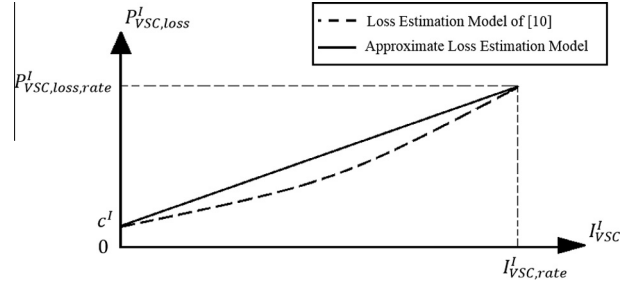

Fig. 2. Comparison between the quadratic and approximate loss estimation function.

Comparing the internal power losses derived from the two models, as shown in Fig. 2, it is noted that when $I_{VSC}^{I} \leqslant I_{VSC,rate}^{I}$, the device power losses using the approximate model are higher than those using the quadratic one, i.e., more conservative conclusions are drawn. The approximate model was used in this paper.

2.2. Optimal operation of Soft Open Points

The benefits of SOPs for both system loss reduction and feeder load balancing were investigated. To quantify these benefits, the amounts of real and reactive power injections of the SOPs were determined through solving a combinational nonlinear constrained optimization problem.

2.2.1. Problem formulation

Two objective functions are used separately to quantify the optimality of the SOP operation.

2.2.1.1. Active power loss minimization.
The active power losses consist of two components: the feeder losses and the internal power losses of the SOP devices. The active power loss minimization problem is formulated as:

$$Minimize \ P_{T,Loss} = \sum_{k=1}^{n_l} r_k \cdot \frac{P_k^2 + Q_k^2}{|V_k|^2} + P_{SOP,Loss} \tag{11}$$

where r_k, P_k, Q_k, V_k are resistance, active power, reactive power, and voltage of branch k; and n_l is the total number of branches in the network.

2.2.1.2. Feeder load balancing.
A branch loading index LI_k is used to measure the loading level of each branch in the network, which is expressed as:

$$LI_k = \left(\frac{I_k}{I_{k,rate}} \right)^2 \ \forall \ k \in n_l \tag{12}$$

where I_k and $I_{k,rate}$ are the actual and the rated branch current of branch k.

Feeder load balancing is achieved by minimizing the load balance index LBI, which is defined as the sum of branch load balancing indices, as shown in (13):

$$Minimize \ LBI = \sum_{k=1}^{n_l} LI_k \tag{13}$$

2.2.1.3. Constraints.
Constraints of the distribution network and the SOP devices are considered. The device constraints of each SOP are shown in (4)–(6). The network constraints are expressed as follows:

$$g(x, s) = 0 \tag{14}$$

$$|V_{i,min}| \leqslant |V_i| \leqslant |V_{i,max}| \; |\forall \; i \in n_b \tag{15}$$

$$|S_k| \leqslant |S_{k,max}| \; \forall \; k \in n_l \tag{16}$$

where $g(x, s), V_{i,min}, V_{i,max}$ and $S_{k,max}$ are the power flow equations, the minimum and the maximum voltage of bus i and the maximum capacity allowed in branch k. n_b are the total number of buses of the network.

2.2.1.4. Penalty function. Constrains of mentioned above are included into the objective function by using the penalty function method. In this way, unconstrained optimization methods are used directly by solving the transformed objective function (with penalty terms):

$$Minimize \; F_{obj}(\mathbf{S}) = \{P_{T,Loss} \; or \; LBI\} + k_1 \cdot f_{SOP} + k_2 \cdot f_V + k_3 \cdot f_S \tag{17}$$

where k_1, k_2, k_3 are the penalty constants; $f_{SOP}, f_V,$ and f_S are the penalty functions for violations of the SOP device constraints, the network voltage and capacity constraints; $\mathbf{S}$ denotes the decision variable vector.

Based on the power injection model of SOP in Section 2.1, the real and reactive power injections at both terminals are specified as the decision variables: with one SOP installation, $\mathbf{S} = \left[P_{S_{inj}}^I, Q_{S_{inj}}^I, Q_{S_{inj}}^J \right]^T$. $P_{S\_inj}^I$ is not included in $\mathbf{S}$ since it is determined directly after $\mathbf{S}$ is specified according to the equality constraint equation of (4). Therefore, the coordinates of n SOPs are combined together sequentially to obtain a point of $\mathbf{S}$ in a $3n$-dimensional space, thus

$$\mathbf{S} = \left[P_{S\_inj,1}^I, Q_{S\_inj,1}^I, Q_{S\_inj,1}^J, P_{S\_inj,2}^I, Q_{S\_inj,2}^I, Q_{S\_inj,2}^J, \dots, P_{S_{inj},n}^I, Q_{S_{inj},n}^I, Q_{S_{inj},n}^J \right]^T \tag{18}$$

2.2.2. Method of determining optimal SOP operation

Based on the Powell's Direct Set (PDS) method presented in [15], an improved PDS method to optimize the SOP operation was developed. The performance improvement is achieved by obtaining a good initial approximated SOP operation.

2.2.2.1. Powell's direct set method. Most mathematical optimization methods require explicit expressions of the derivatives to define the direction of movement, i.e. search direction approaching to the optimum (from a starting point).

The Powell's Direct Set method is a direct search method proposed by Powell [15]. It defines the search directions in a direct manner, i.e., solely depending on the objective function itself. Therefore, this method is easy to implement and is not limited by the existence of derivatives of the objective function. It has been successfully applied to solve problems for which it is difficult or impossible to calculate the derivatives [16–18].

A comprehensive review of PDS method as well as the mathematical proof of its convergence were given in [15]. Three key properties of this method are highlighted below:

(i) For an N-dimensional problem, minimization is achieved by an iterative procedure that searches down N linear independent directions within each iteration, i.e. starting from the best known approximation to the optimum.
(ii) Fast convergence to the optimum is achievable by only searching down N mutually conjugate directions. The optimal solution of a quadratic function has been proved achievable by searching along those mutually conjugate directions once only. Hence only N iterations are required to solve the

N-dimensional quadratic problem [15]. The efficacy has also been demonstrated for any other function form, as presented in [16,17], but may require more iterations.
(iii) The mutually conjugate directions are generated after each iteration, as illustrated in the following part.

2.2.2.2. PDS method for optimal SOP operation. The process of determining optimal SOP operation using the PDS method is shown in Fig. 3:

Step 1: Initialization. Based on (19), the initial approximate SOP operation $\mathbf{S}_0^{(1)}$, the initial search direction set with $3n$ linear independent search directions, $\{\xi\}^{(1)} = \{\xi_1^{(1)}, \dots, \xi_i^{(1)}, \dots, \xi_{3n}^{(1)}\}$ and the convergence criterion ε are specified. The $3n$ directions in $\{\xi\}^{(1)}$ are initially chosen to be the co-ordinate directions (linear independent). This means only one decision variable in (19) will be changed when searching along one direction.

Step 2: Generate a new mutually conjugate direction within one iteration. There are two sub steps:

– starting from $\mathbf{S}_0^{(k)}$, k indicates the iteration number (one iteration includes searching along $3n$ directions, $k = 1$ initially), sequentially find $\mathbf{S}_i^{(k)}$ which gives the minimum of the objective function (17) along each search direction, $\xi_i^{(k)}$ in $\{\xi\}^{(k)}$, which is expressed as:

$$Min \; F_{obj}\left(\mathbf{S}_i^{(k)}\right) = F_{obj}\left(\mathbf{S}_{i-1}^{(k)} + \lambda_i \cdot \xi_i^{(k)}\right), \quad i = 1, 2, \dots, 3n \tag{19}$$

In this paper, a one-dimensional search method, the Golden Ratio Rule method [19], was adopted to calculate the optimal step size, λ_i.
The load flow analysis method introduced in [5] combined with the SOP injection model formulated in (1)–(4) was implemented as a subroutine to calculate the objective function $F_{obj}(\mathbf{S}_i^{(k)})$ in (19).

– after searching down the $3n$ directions, a conjugate direction is generated by (20)

$$\xi_{conju.}^{(k)} = \mathbf{S}_{3n}^{(k)} - \mathbf{S}_0^{(k)} \tag{20}$$

Step 3: Update the search direction set for the next iteration $\{\xi\}^{(k+1)}$. Two scenarios are considered:

– If $n = 1$, discard the first direction $\xi_1^{(k)}$ in $\{\xi_i^{(k)}\}$ by adding $\xi_{conju.}^{(k)}$ to the end, as shown in (21)

$$\{\xi\}^{(k+1)} = \left\{ \xi_2^{(k)}, \xi_3^{(k)}, \dots, \xi_{3n}^{(k)}, \xi_{conju.}^{(k)} \right\} \tag{21}$$

– If $n > 1$, a 'smarter' updating procedure is required to ensure a reasonable rate of convergence, i.e. replace the direction in $\{\xi\}^{(k)}$, which shows the worst performance. The general procedure is presented as follows [15]:
• Find $\xi_m^{(k)}$ that gives maximum reduction among the previous one-dimensional searching processes in Step 2, as shown in (22):

$$\Delta_{max} = \max_{1 \leqslant m \leqslant 3n} \left\{ F_{obj}\left(\mathbf{S}_{m-1}^{(k)}\right) - F_{obj}\left(\mathbf{S}_m^{(k)}\right) \right\} \tag{22}$$

• Replace $\xi_m^{(k)}$ by $\xi_{conju.}^{(k)}$ giving more efficient convergence if the following two criterions are satisfied
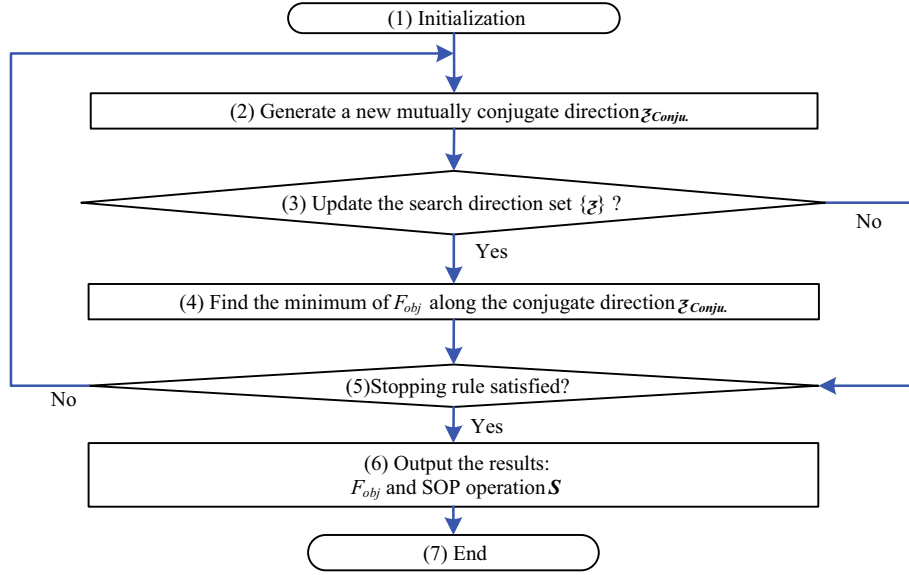
Fig. 3. Flow chart of the proposed PDS method.

$$\left.\begin{array}{c}(w_1 - 2w_2 + w_3)(w_1 - w_2 - \Delta_{max})^2 < 0.5 \cdot \Delta_{max}(w_1 - w_3)^2 \\ w_3 < w_1\end{array}\right\} \tag{23}$$

where $w_1 = F_{obj}\left(\boldsymbol{S}_0^{(k)}\right)$, $w_2 = F_{obj}\left(\boldsymbol{S}_{3n}^{(k)}\right)$, $w_3 = F_{obj}\left(2 \cdot \boldsymbol{S}_{3n}^{(k)} - \boldsymbol{S}_0^{(k)}\right)$. Thus,

$$\{\xi\}^{(k+1)} = \left\{\xi_1^{(k)}, \ldots, \xi_{m-1}^{(k)}, \xi_{conju.}^{(k)}, \xi_{m+1}^{(k)}, \ldots, \xi_{3n}^{(k)}\right\} \tag{24}$$

- Otherwise $\{\xi\}^{(k)}$ is not updated in this iteration, let $\boldsymbol{S}_0^{(k+1)} = \boldsymbol{S}_{3n}^{(k)}$ and jump to Step 5.

An example shown in Fig. 4 illustrates the searching of the optimization process. As the red[1] solid line shows, the optimization starts from an initial approximation $\boldsymbol{S}_0^{(1)}$ and then reaches the minimum $\boldsymbol{S}_1^{(1)}, \boldsymbol{S}_2^{(1)}, \boldsymbol{S}_3^{(1)}$ along each of the coordinate directions in $\{\xi\}^{(1)}$. The first conjugate direction $\xi_{conju.}^{(1)}$ is hence obtained, as shown by the blue dotted arrow. After searching along the conjugate direction, a new approximation $\boldsymbol{S}_0^{(2)}$ is obtained for the second iteration.

2.2.2.3. Determine the initial approximated SOP operation. The PDS method is able to start from any initial point $\boldsymbol{S}_0^{(1)}$. A good approximation of SOP operation is obtained by running the PDS method once using the objective function of (19) with simplified power flow equations given by [5]:

(i) All nodal voltage magnitudes are assumed to be 1 p.u., Eqs. (11) and (13) are reduced to

$$P_{Loss} \approx \sum_{k=1}^{n_l} r_k \cdot \left(P_k^2 + Q_k^2\right) + P_{SOP,Loss} \tag{25}$$

$$LIB \approx \sum_{k=1}^{n_l} \frac{P_k^2 + Q_k^2}{I_{k,rate}^2} \tag{26}$$

---

[1] For interpretation of color in Fig. 4, the reader is referred to the web version of this article.
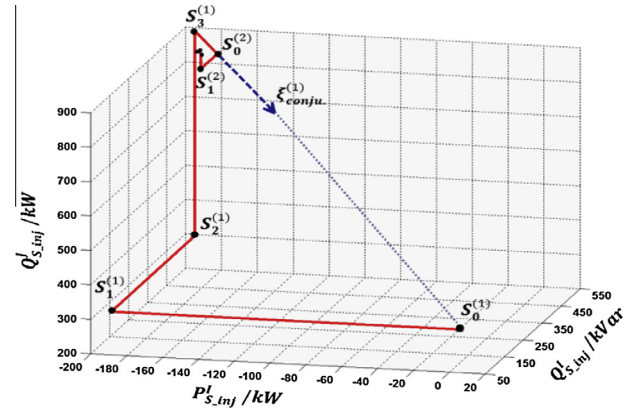

Fig. 4. Example of one SOP optimization by PDS method.

(ii) Ignoring all the quadratic terms (line losses) from the power flow equations in (1). The branch power P_k and Q_k are obtained by summing up the downstream power loads:

$$P_k \approx \sum_{i=k+1}^{n} P_{L,i} \tag{27}$$

$$Q_k \approx \sum_{i=k+1}^{n} Q_{L,i} \tag{28}$$

The constraints of nodal voltage and branch capacity are considered by:

$$|V_i|^2 \approx |V_0|^2 - 2\sum_{k=1}^{i}(r_k P_k + x_k Q_k) \leqslant V_{max}^2 \tag{29}$$

$$S_k \approx \left(P_k^2 + Q_k^2\right) \leqslant S_{k,max}^2 \tag{30}$$

Using the simplified equations, as shown in (25)–(30), the initial approximated SOP operation is obtained directly without using the accurate load flow calculations.

2.3. Network reconfiguration considering SOPs

Reconfiguring distribution networks is used to achieve better network operation including power loss minimization, feeder load balancing and supply restoration. To investigate the performance of distribution network reconfiguration when SOPs are installed to replace some of the normally-open points, the proposed PDS method for optimal SOP operation was combined with the network reconfiguration method introduced in [20].

The procedure of the combined algorithm is given in Fig. 5. According to [20], a shortest-path algorithm is used to find the optimal electricity supply path for each load busbar. A genetic algorithm (GA) with the selection, crossover and mutation operators is used to optimize the sequence of load busbars searching for the supply paths because the sequence affects the obtained network configurations. The improved PDS method for optimal SOP operation is integrated after the shortest path algorithm. The fitness functions utilized are formulated in Section 2.2.

3. Case study

A 33-bus distribution network, as shown in Fig. 6, was used for case study [5]. This network has 32 normally-closed switches, 5 normally-open switches and the nominal voltage is 12.66 kV. The total real and reactive power loads are 3715 kW and 2300 kVar. Four normally-open switches, i.e., the switches between buses 25 and 29, 33 and 18, 8 and 21, 12 and 22, are chosen as candidate places for SOP installation. The capacity limit of each SOP unit is 3 MVA.

Four cases were defined and used for quantifying the benefits of SOPs for improvement of network performance:

Case I: Improve network performance using SOPs.
Case II: Improve network performance considering both SOPs and network reconfiguration.
Case III: Impact of DG connections.
Case IV: Impact of power losses of SOP devices.

3.1. Improve network performances using SOPs

The impact of different number of SOPs installed in the network on both power loss minimization and feeder load balancing was investigated. The device power losses were ignored for this case.

3.1.1. Power loss minimization

Fig. 7a shows the results of minimized power losses with 1–4 SOPs installed in the network. There was a significant reduction (by 42%) of the system power loss with one SOP installation. With more SOPs installed in the system, the total power losses were
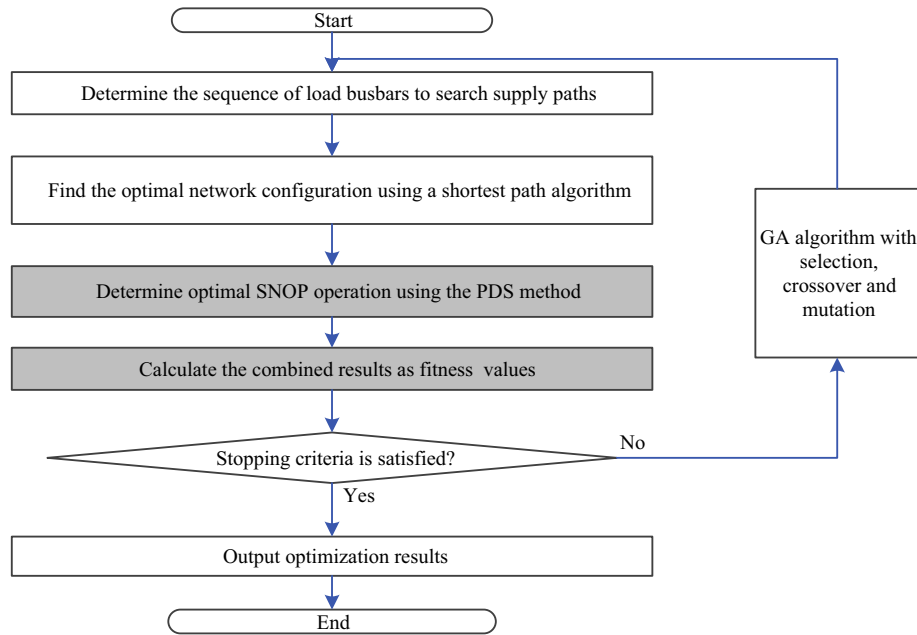

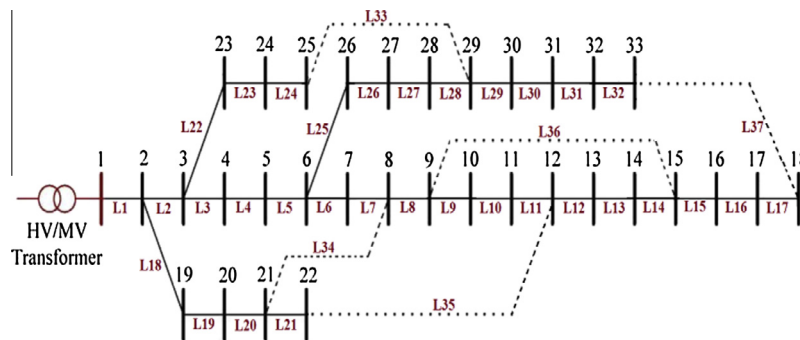Fig. 5. Flowchart of proposed network reconfiguration considering SOPs.

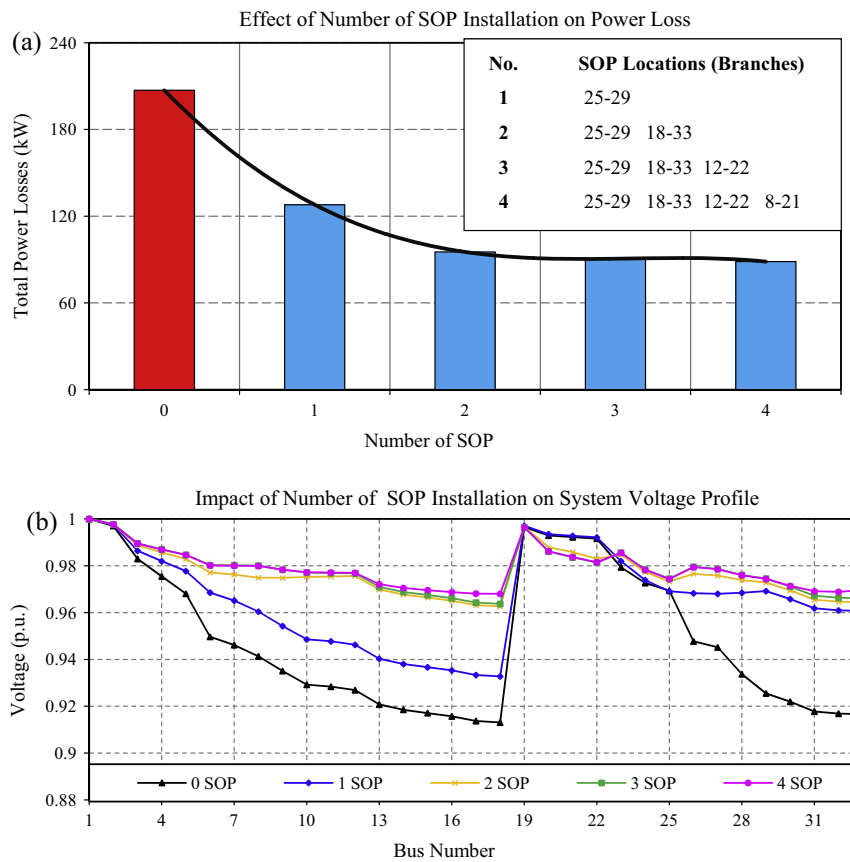
Fig. 6. 33-bus distribution network.

Fig. 7. Impact of different number of SOP installation on power loss minimization and voltage profile improvement.
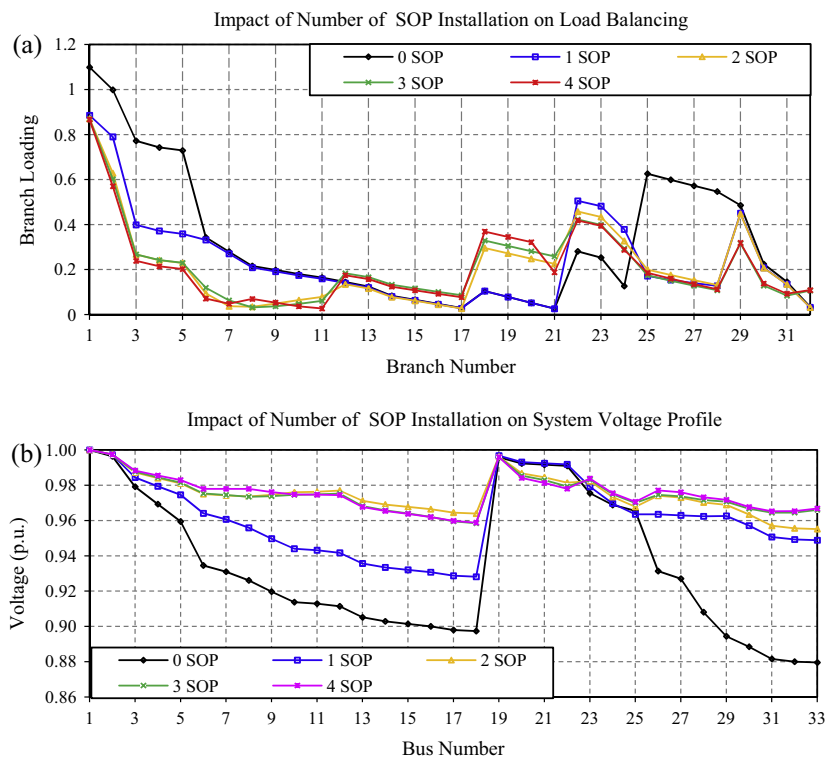

Fig. 8. Impact of different number of SOP installation on load balancing and voltage profile improvement.

Table 1
System load balancing index with different number of SOP installation.

Number of SOP installed	0	1	2	3	4
SOP locations (branches)	–	25–29	25–29 18–33	25–29 18–33 12–22	25–29 18–33 12–22 8–21
System load balancing index	6.156	3.218	2.566	2.428	2.389
% *LBI* reduction	–	47.726	58.317	60.056	61.192

further reduced (by 57%). The voltage profiles of the system were also improved with the SOP installations, as shown in Fig. 7b.

3.1.2. Feeder load balancing

One feeder of the network from branch L25 to branch L32 as shown in Fig. 8 was assumed to be heavily loaded, i.e., 1.6 times higher than the loading under the normal condition. Table 1 shows the impact of different number of SOPs on feeder load balancing. It is observed that the system load balancing index *LBI* was reduced by 47.73% with one SOP. Although the *LBI* reduction was further improved with more SOPs installed, the rate of improvement was diminishing. Fig. 8a illustrates the branch loading profile of the network. By using SOPs, the loading of those heavily loaded branches (e.g. branches L1 to L6 and L25 to L30) was reduced dramatically by transferring loads to the lightly loaded branches via SOP control. As a consequence, the loading levels from branches L12 to L24 were increased. The voltage profile was also improved,

as shown in Fig. 8b. The minimum bus voltage (at bus 32) was 0.88 p.u. due to overloading, and it was improved by 9.09% after the system loading was balanced using SOPs.

The results also show that beyond two SOPs, the benefits of loss minimization, load balancing and voltage regulation are not increased significantly. Therefore, the proposed method can be used to derive the optimum amount of SOPs for a given network.

3.1.3. Performance of the improved PDS method for optimal SOP operation

The effectiveness of the proposed method with a good initial approximation was evaluated in this case study. Table 2 lists the computation time required for the calculation of above case studies considering only one SOP. The total time required by using the conventional PDS method (starting from an arbitrary point) and the proposed method with a good initial approximation were compared. It can be seen that for both power loss minimization and feeder load balancing there were significant reductions in computation time by using the improved PDS method. Especially for solving the feeder load balancing, the total CPU time required was reduced by 68% (from 8.295 s to 2.614 s) after using the improved PDS method.

3.2. Improve network performance considering both SOP and network reconfiguration

The benefits of combining SOP and network reconfiguration for power loss minimization and feeder load balancing were evaluated. In this case, the SOP device was assumed to be located

Table 2
Results of computing time for optimal SOP operation.

Optimization technique	Power loss minimization			Feeder load balancing		
		PDS	Improved PDS		PDS	Improved PDS
CPU time (s)	Light Loading	4.565	1.998	Overload condition	8.295	2.614
	Normal Loading	5.364	3.343			
	Heavy Loading	5.774	3.578			

Table 3
Results of different methods for power loss minimization.

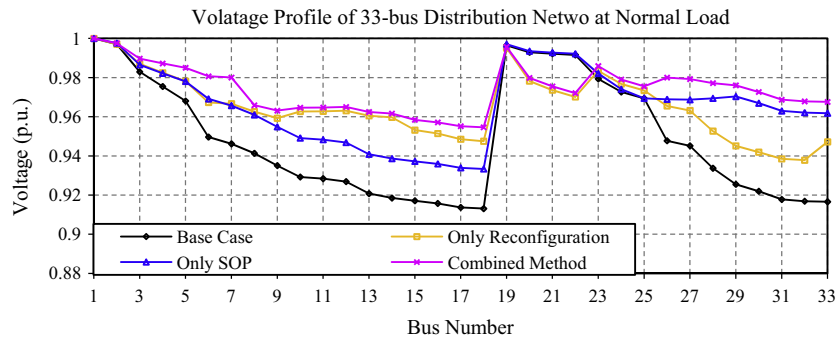| Case studies			Load Level		
			Light (50%)	Normal (100%)	Heavy (160%)
Base case	Switches with open status		8–21 12–22 25–29 9–15 18–33		
No reconfiguration	Power loss (kW)		47.118	202.876	575.966
No SOP installed	Minimum voltage (p.u.)		0.958	0.913	0.853
Only network reconfiguration	Switches opened		7–8 9–10 14–15 25–29 32–33		
	Power loss (kW)		33.312	137.946	381.418
	% Loss reduction		29.301	32.005	33.778
	Minimum voltage (p.u.)		0.970	0.938	0.897
Only SOP	Switches with open status		8–21 12–22 9–15 18–33		
	SOP operation	$P^1_{S\_inj}$ (MW)	0.230	0.605	0.998
		$Q^1_{S\_inj}$ (MVar)	0.225	0.471	0.784
		$Q^2_{S\_inj}$ (MVar)	0.610	1.239	2.017
	Power loss (kW)		29.774	124.456	337.525
	% Loss reduction		36.810	38.653	41.398
	Minimum voltage (p.u.)		0.967	0.933	0.890
Combined network reconfiguration with SOP	Switches with open status		7–8 9–10 14–15 18–33		
	SOP operation	$P^1_{S\_inj}$ (MW)	0.183	0.374	0.607
		$Q^1_{S\_inj}$ (MVar)	0.215	0.424	0.697
		$Q^2_{S\_inj}$ (MVar)	0.516	1.045	1.686
	Power loss (kW)		22.758	93.915	250.179
	% Loss reduction		51.700	53.708	56.564
	Minimum voltage (p.u.)		0.978	0.955	0.925

Fig. 9. Voltage profiles of the network under normal loading condition.

Table 4
Results of different methods for load balancing.

Case studies		Base case	Only network reconfiguration	Only SOP	Combined reconfiguration with SOP
System load balancing index		6.156	4.139	3.218	2.594
% LBI reduction		–	32.765	47.726	68.337
Minimum voltage (p.u.)		0.880	0.904	0.928	0.943
SOP operation	$P_{S\_inj}^1$ (MW)	–	–	0.916	1.142
	$Q_{S\_inj}^1$ (MVar)	–	–	0.569	0.577
	$Q_{S\_inj}^2$ (MVar)	–	–	1.791	2.417

between buses 25 and 29 and its power losses were ignored. Three case studies were also carried out for comparisons, which are base case study with neither reconfiguration nor SOP; case study considering only network reconfiguration; and case study considering only one SOP, which is located between buses 25 and 29.

3.2.1. Power loss minimization

The network performance on power loss minimization was simulated under three loading conditions: light (50%), normal (100%),

and heavy (160%). The simulation results are listed in Table 3. The percentages of total power loss reduction implies that using only one SOP achieved a similar power loss reduction to that of network reconfiguration under three loading conditions. The most significant power loss reductions and voltage improvement under all three loading conditions were obtained using the combined method. The SOP operation required to achieve power loss minimization indicates that the combined method contributed more to power loss reduction while requiring smaller SOP sizes. Fig. 9
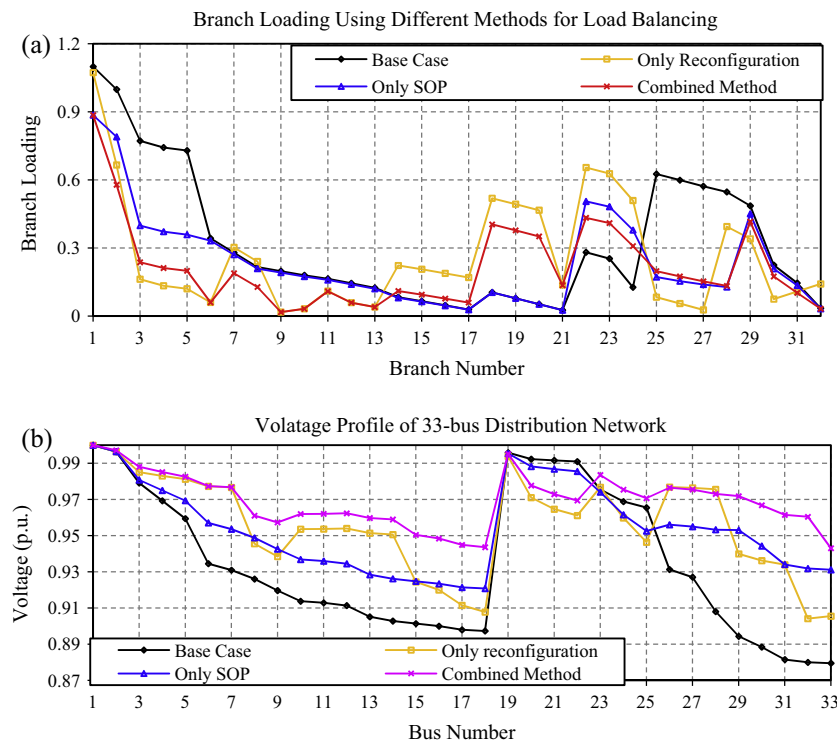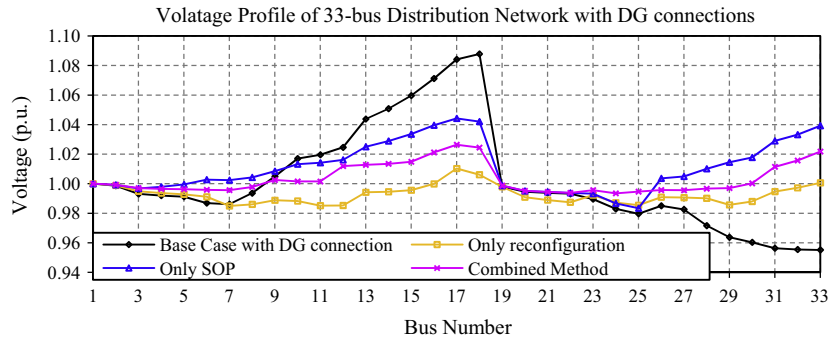

Fig. 10. Results of load balancing capability and relevant voltage profile improvement under different methods.

Table 5
Results of different methods for power loss minimization with DG connections.

Case studies		Base case without DGs	Base case with DGs	Only network reconfiguration	Only SOP	Combined reconfiguration with SOP
Total power losses (kW)		202.875	345.502	120.783	92.334	63.221
% Loss reduction		–	–	65.044	73.275	81.702
SOP operation	$P_{S\_inj}^1$ (MW)	–	–	–	1.661	1.606
	$Q_{S\_inj}^1$ (MVar)	–	–	–	0.376	0.381
	$Q_{S\_inj}^2$ (MVar)	–	–	–	0.899	0.904

Fig. 11. Voltage profiles of the network under different cases with DG connections.

illustrates the voltage profiles of all case studies under the normal loading condition. The shapes of the voltage profile under the other two loading condition were the same except minor change in magnitude, and hence are not illustrated in the paper.

3.2.2. Feeder load balancing

The same overloading condition described in the previous case study was simulated. Table 4 presents the load balancing index for the four case studies. The branch loading profiles and voltage profiles are shown in Fig. 10. From these results, it is seen that by using only one SOP to control network power flows achieved better performance on load balancing than that of using network reconfiguration to change the open/close status of a sequence of switches. The highest LBI reduction, i.e., the most well-balanced network, and the highest improvement on minimum voltage were achieved using the combined method.

3.3. Impact of DG connections

A large capacity of intermittent renewable energy in the distribution network can increase feeder loads unbalance and network power losses. To evaluate the benefits of using the SOP for power loss minimization and feeder load balancing with DG connections, three DGs were assumed to be connected to buses 16, 17 and 18. Each DG had a power production of 1 MW with a unity power factor and was modeled as a negative load in this study. An SOP was assumed to be located between buses 18 and 33 and its power losses were ignored. Five case studies were carried out for comparisons, which are base case study with and without DG connections;

case study using only network reconfiguration; case study using only one SOP; and case study using the combined network reconfiguration and SOP.

3.3.1. Power loss minimization

Table 5 shows that network power losses for the five case studies under normal loading conditions. It can be seen that the network power losses were increased by 70% due to the DG connections. A significant power loss reduction (72%) was achieved by using only one SOP, which gave better performance than by using only network reconfiguration. The most significant power loss reduction was obtained by using the combined method while requiring smaller SOP size. Fig. 11 shows the voltage profile of the network. There was a notable voltage rise due to the DG connections. By using the SOP (either with or without network reconfiguration) achieved much flattered network voltage profile.

3.3.2. Feeder load balancing

To evaluate the benefits of the SOP for feeder load balancing with DG connections, especially when one feeder has high DG power generation while the other one is under a heavy loading condition, the same overloading condition adopted previously was used again. Table 6 shows the load balancing index for the five case studies. It is observed that the network was more unbalanced (higher LBI) after connecting DGs. A significant reduction on LBI (77.51%) was achieved by transferring loads from the heavily loaded feeder to that with DG integration via the SOP, which gave much better performance than that by changing the open/close

Table 6
Results of different methods for load balancing with DG connections.

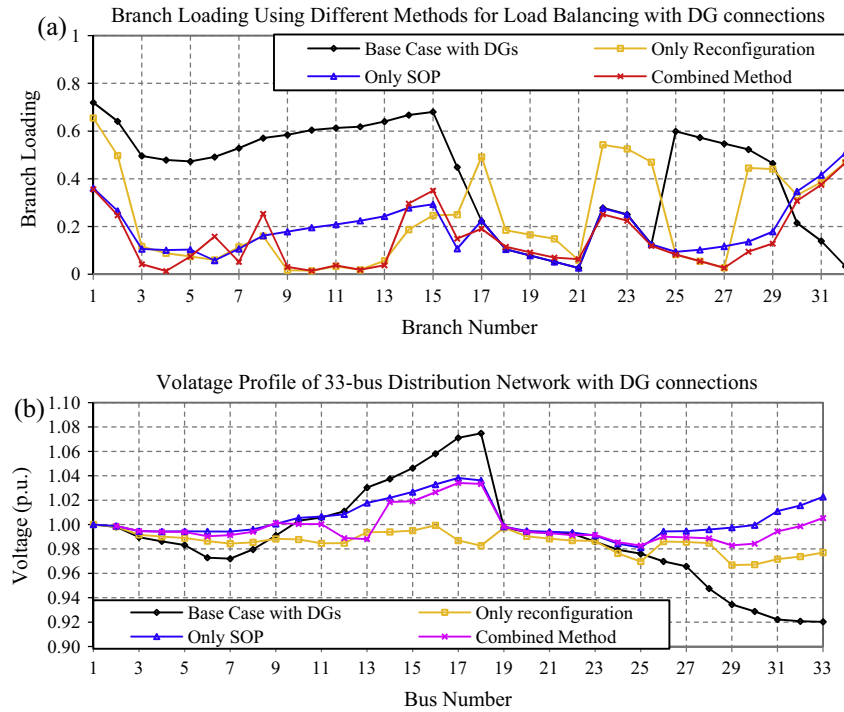| Case studies		Base case without DGs	Base case with DGs	Only network reconfiguration	Only SOP	Combined reconfiguration with SOP
System load balancing index		6.156	7.238	2.995	1.628	1.267
% LBI reduction		–	–	58.621	77.507	82.495
SOP operation	$P_{S\_inj}^1$ (MW)	–	–	–	1.692	1.480
	$Q_{S\_inj}^1$ (MVar)	–	–	–	0.457	0.523
	$Q_{S\_inj}^2$ (MVar)	–	–	–	1.252	1.211

Fig. 12. Results of load balancing capability and relevant voltage profile improvement under different cases with DG connections.

switch status via network reconfiguration. The most well-balanced network was achieved by using the combined method with smaller SOP size required. Fig. 12 shows the branch loading profiles and voltage profiles. As shown in Fig. 12a, the peak branch loading of the network was reduced from 72% to 50% by using only one SOP. It shows that the increase in peak currents in the feeders and branch loading was reduced effectively by only using one

SOP. The combined method achieved the lowest peak branch loading. The voltage profile was also much flatter by using the SOP and the combined method, as shown in Fig. 12b.

This study considered only balanced 3-phase feeders. However the proposed method is also applicable for unbalanced 3-phase distribution networks where 3-phase unbalanced power flow analysis needs to be employed.
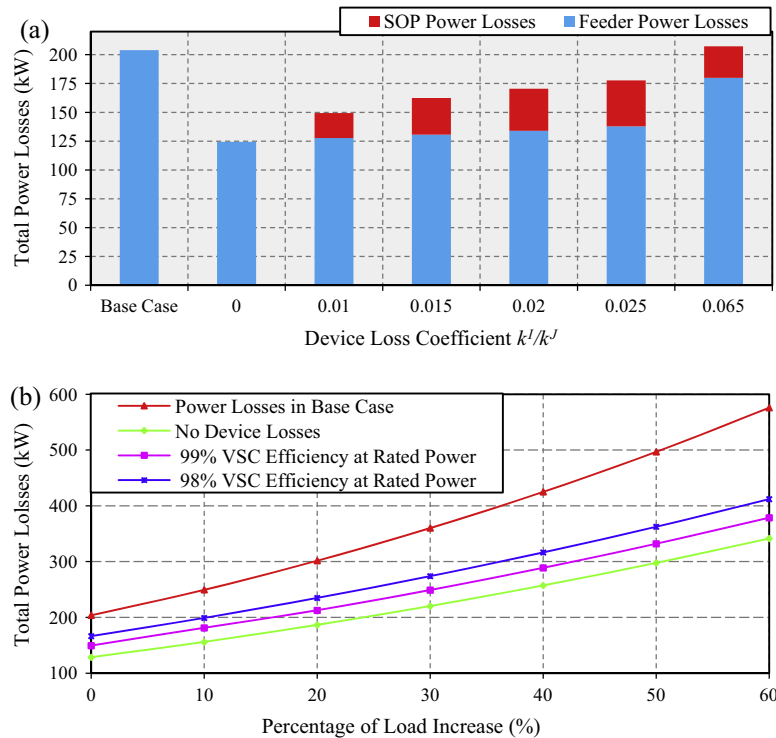

Fig. 13. Impacts of the SOP device losses on total network power losses.

3.4. Impact of the SOP device losses

A significant reduction on feeder power losses using SOPs has been demonstrated in the previous study, where the SOP device losses were not considered. Although the SOP device losses have minor impact on its power flow control, it may lower the economic benefits obtained from reducing the total network power losses. The impact of SOP device losses on the total network power loss reduction was investigated based on sensitivity analysis. Different VSC efficiencies at the rated power, i.e. the values of loss coefficients k^I and k^J in (9), were considered. Here for the VSCs in the back-to-back converters, it was assumed that k^I is equal to k^J. The constant power loss of each SOP device was set as 0.2% of the rated power.

Fig. 13a illustrates the total network power loss minimization (feeder losses and SOP device losses) under the normal loading conditions using one SOP which is located between buses 25 and 29 (without DG connections). Different device efficiencies of each VSC were considered from 93.5% to 100%. It is observed that the total network losses were able to be reduced by using the SOP. However, the benefits were lowered when the device efficiency decreased. The SOP lost its capability in reducing network power losses when the device loss coefficients fell to 0.065, i.e., 93.5% VSC efficiency at the rated power. Fig. 13b shows the performance on total network power losses for each percentage of system loading increase from 0% to 60%. The figure shows that SOP had a greater positive impact on the network power losses under higher system loading conditions. The requirements on SOP device efficiency for total network loss reduction were reduced when the system loading increases.

4. Conclusions

The benefits of using SOPs for medium voltage distribution networks were investigated focusing on power loss reduction, feeder load balancing and voltage profile improvement. A generic power injection model of SOP that is suitable for steady state analysis was developed, taking into account both physical limits and internal power losses of a typical SOP device: back to back voltage source converters. The optimal SOP operation is obtained using improved Powell's Direction Set method and the combined method considering both SOP and network reconfiguration was proposed to demonstrate the superiority of using SOPs. Different quantity of SOPs were considered and showed that SOPs contributed to significant power loss reduction, feeder load balancing and voltage profile improvement. By comparing with network reconfiguration, using only one SOP achieved similar improvement on network power loss reduction and feeder load balancing. The greatest improvements were obtained when combining SOP and network reconfiguration where smaller SOP sizes were required. High penetration of DGs in the distribution network increases the needs for loss minimization and feeder load balancing. Using only one SOP achieved better performance than using network reconfiguration. Combining SOP and network reconfiguration contributed to the greatest improvements. In addition, SOPs are able to significantly reduce the peak currents in feeders and alleviate undesirable voltage excursions induced by the connection of DG and demand. Therefore SOPs can be used as an alternative to infrastructure upgrades in accommodating distributed energy resources. The impact of SOP device losses was illustrated which shows that the economic benefit of SOP obtained from reducing total network power losses was lowered with the decrease of device efficiency.

However, a greater positive impact was obtained when system loading increased. The requirements on SOP device efficiency for total network loss reduction were reduced when the system loading increases.

Although the focus of this paper is to quantify the technical benefits of SOPs, the proposed algorithm is also able to be used for further economic analysis and planning studies of the application of SOPs, where life cycle costs need to the quantified and the optimal amount, locations and sizes of SOPs need to be determined considering the capital cost of SOPs.

References

[1] Hung DQ, Mithulananthan N, Bansal RC. Integration of PV and BES units in commercial distribution systems considering energy loss and voltage stability. Appl Energy 2014;113:1162–70.

[2] Mu Y, Wu J, Jenkins N, Jia H, Wang C. A spatial-temporal model for grid impact analysis of plug-in electric vehicles. Appl Energy 2014;114:456–65.

[3] Järventausta P, Repo S, Rautiainen A, Partanen J. Smart grid power system control in distributed generation environment. Annu Rev Control 2010;34:277–86.

[4] Enacheanu B, Raison B, Caire R, Devaux O, Bienia W, HadjSaid N. Improving voltage profile of residential distribution systems using rooftop PVs and battery energy storage systems. Appl Energy 2014;134:290–300.

[5] Baran ME, Wu FF. Network reconfiguration in distribution systems for loss reduction and load balancing. IEEE Trans Power Deliv 1989;4:1401–7.

[6] Kechroud A, Myrzik JMA, Kling W. Taking the experience from flexible AC transmission systems to flexible AC distribution systems. In: 42nd International universities power engineering conference; 2007. p. 687–92.

[7] Mutale J, Strbac G. Transmission network reinforcement versus FACTS: an economic assessment. In: IEEE power industry computer applications conference; 1999. p. 961–67.

[8] Bloemink JM, Green TC. Increasing distributed generation penetration using soft normally-open points. In: IEEE power and energy society general meeting; 2010. p. 1–8.

[9] Bloemink JM, Green TC. Benefits of distribution-level power electronics for supporting distributed generation growth. IEEE Trans Power Deliv 2013;28:911–9.

[10] Sayed MA, Takeshita T. All nodes voltage regulation and line loss minimization in loop distribution systems using UPFC. IEEE Trans Power Electron 2011;26:1694–703.

[11] Okada N, Takasaki M, Sakai H, Katoh S. Development of a 6.6 kV–1 MVA transformerless loop balance controller. In: IEEE power electronics specialists conference; 2007. p. 1087–91.

[12] Baran ME, Wu FF. Optimal sizing of capacitors placed on a radial distribution system. IEEE Trans Power Deliv 1989;4:735–43.

[13] Flourentzou N, Agelidis VG, Demetriades GD. VSC-based HVDC power transmission systems: an overview. IEEE Trans Power Electron 2009;24:592–602.

[14] Daelemans G, Srivastava K, Reza M, Cole S, Belmans R. Minimization of steady-state losses in meshed networks using VSC HVDC. In: IEEE power and energy society general meeting; 2009. p. 1–5.

[15] Powell MJD. An efficient method for finding the minimum of a function of several variables without calculating derivatives. Comput J 1964;7:155–62.

[16] Cheng-Ling L, Tai-Ning C, Yuan-Yao L, Pin H, Lee RK. Powell's method for designing optical multilayer thin-film filters. In: Optoelectronics and communications conference; 2010. p. 388–89.

[17] Lazarou S, Vita V, Ekonomou L. Application of Powell's optimisation method for the optimal number of wind turbines in a wind farm. IET Sci Measur Technol 2011;5:77–80.

[18] Cho H, Smith AD, Mago P. Combined cooling, heating and power: a review of performance improvement and optimization. Appl Energy 2014;136:168–85.

[19] Kiefer J. Sequential minimax search for a maximum. Proc Am Math Soc 1953;4:502–6.

[20] Yu Y, Wu J. Loads combination method based core schema genetic shortest-path algorithm for distribution network reconfiguration. In: Proceedings of power system technology conference, vol. 3; 2002. p. 1729–33.